[10] A. Rajca, A. Safronov, S. Rajca, R. Schoemaker, *Angew. Chem.* **1997**, *109*, 504–507; *Angew. Chem. Int. Ed. Engl.* **1997**, *36*, 488–491; A. Rajca, A. Safronov, S. Rajca, J. Wongsriratanakul, *J. Am. Chem. Soc.* **2000**, *122*, 3351–3357.

[11] 4,4′-Dibromo-3,3′-bithienyl (**2**): S. Gronovitz, *Acta Chem. Scand.* **1961**, *15*, 1393–1395.

[12] Dithieno[2,3-*b*:3′,2′-*d*]thiophene and bis(phenylsulfonyl)sulfide: F. de Jong, M. J. Janssen, *J. Org. Chem.* **1971**, *36*, 1645–1648.

[13] Crystal data for **1**, containing a disordered molecule of chloroform: colorless needle, $0.35 \times 0.06 \times 0.04$ mm, $C_{23}H_{19}Br_2Cl_3S_7Si_2$, $M =$ 842.15, trigonal, $a = b = 36.319(2)$ Å, $c = 12.8012(8)$ Å, $V =$ 14623(2) Å$^3$, $T = 173(2)$ K, space group $R\bar{3}$, $Z = 18$, $\rho_{calcd} =$ 1.721 Mg m$^{-3}$, $\mu = 3.281$ mm$^{-1}$, $2\theta_{max} = 55$, $Mo_{K\alpha}$ ($\lambda = 0.71073$). A total of 50542 reflections were measured, of which 7463 ($R_{int} = 0.073$) were unique. The included solvent molecule, chloroform, is statistically disordered over two positions. Final residuals were $R = 0.0370$ and $wR2 = 0.0857$ (for 5083 observed reflections with $I > 2\sigma(I)$, 352 parameters) with GOF 0.965 and largest residual peak 1.049 e Å$^{-3}$ and hole $-1.181$ e Å$^{-3}$. Crystal data for **4**: colorless block, $0.35 \times 0.21 \times 0.20$ mm, $C_{14}H_{18}Br_2S_3Si_2$, $M = 498.46$, orthorhombic, $a =$ 10.0656(7), $b = 11.2301(8)$, $c = 35.400(3)$ Å, $V = 4001.5(5)$ Å$^3$, $T =$ 173(2) K, space group $Pbca$, $Z = 8$, $\rho_{calcd} = 1.655$ Mg m$^{-3}$, $\mu =$ 4.476 mm$^{-1}$, $2\theta_{max} = 55.06$, $Mo_{K\alpha}$ ($\lambda = 0.71073$). A total of 39332 reflections were measured, of which 4596 ($R_{int} = 0.041$) were unique. Final residuals were $R = 0.0305$ and $wR2 = 0.0741$ (for 3701 observed reflections with $I > 2\sigma(I)$, 262 parameters) with GOF 1.068 and largest residual peak 0.628 e Å$^{-3}$ and hole $-0.468$ e Å$^{-3}$. All data were collected on a SMART Platform CCD (Bruker) equipped with a low temperature device (Oxford cryostream). The intensity data were corrected for absorption (SADABS, R. Blessing, *Acta Crystallogr. Sect. A* **1995**, *51*, 33–38). Final cell constants were calculated from 8192 (for **1**) and 6423 (for **4**) strong reflections from the dataset (SAINT, Bruker Analytical Systems, Madison, WI, **1999**). The structures were solved using direct methods (SIR92, A. Altomare, G. Cascarno, C. Giacovazzo, A. Gualardi, *J. Appl. Cryst.* **1993**, *26*, 343–350) and refined by full-matrix least-square/difference Fourier cycles (SHELXTL V5.10, Bruker Analytical X-Ray Systems, Madison, WI). All non-hydrogen positions were refined anisotropically. All hydrogen atoms were refined isotropically as a riding model. Crystallographic data (excluding structure factors) for the structures reported in this paper have been deposited with the Cambridge Crystallographic Data Centre as supplementary publication no. CCDC-149503 (**1**) and -149502 (**4**). Copies of the data can be obtained free of charge on application to CCDC, 12 Union Road, Cambridge CB2 1EZ, UK (fax: (+44) 1223-336-033; e-mail: deposit@ccdc.cam.ac.uk).

[14] In **4**, the mean deviation from a calculated least-square plane including all the thiophene rings (S1–S3, C1–C8) is 0.0034 Å.

[15] I. Navaza, G. Tsoucaris, G. Le Bas, A. Navaza, C. de Rango, *Bull. Soc. Chim. Belg.* **1979**, *88*, 863–870.

[16] The inner helix climbs and in-plane turns for each thiophene (and benzene) ring are as follows: for **1**, 0.635 Å (36.6°), 0.501 Å (36.9°), 0.292 Å (38.2°), reference plane (38.1°), 0.286 Å (37.9°), 0.539 Å (37.4°), 0.668 Å (34.9°), and for [6]helicene, 0.696 Å (58.2°), 0.648 Å (49.5°), 0.201 Å (52.8°), 0.189 Å (53.0°), 0.622 Å (50.4°), 0.765 Å (54.0°). For [6]helicene, the reference plane includes the two carbons on the middle (approximate twofold) axis and the four nearest-neighbor carbons. Mean deviation from plane is 0.134 Å.

[17] UV/Vis ($CH_2Cl_2$): $\lambda_{max}$[nm] ($\lg(\varepsilon_{max}$[L mol$^{-1}$ cm$^{-1}$])) = 235 (4.55, sh), 256 (4.65), 276 (4.60, sh) for **1**; 236 (4.59), 266 (4.27), 274 (4.25, sh) for **4**.

[18] Cross-conjugated systems: Y. Zhao, R. R. Tykwinski, *J. Am. Chem. Soc.* **1999**, *121*, 458–459; S. Eisler, R. R. Tykwinski, *Angew. Chem.* **1999**, *111*, 2138–2141; *Angew. Chem. Int. Ed.* **1999**, *38*, 1940–1943; T. M. Londergan, Y. You, M. E. Thompson, W. P. Weber, *Macromolecules* **1998**, *31*, 2784–2788.

# Towards the DRED of Resin-Supported Combinatorial Libraries: A Non-Invasive Methodology Based on Bead Self-Encoding and Multispectral Imaging**

Hicham Fenniri,* Hartmut G. Hedderich, Kenneth S. Haber, Jihane Achkar, Brian Taylor, and Dor Ben-Amotz

Combinatorial synthetic methods allow for the preparation of large arrays of compounds as mixtures or individual entities. In the latter case, split synthesis has proven to be ideal in maximizing the number of compounds generated per synthetic step.[1] While the composition of chemical libraries produced using this method is predictable with a high level of confidence, the structural elucidation of potent member(s) after an activity assay remains a challenge. To unravel the chemical nature of the active members several tactics based on encoding methodologies[2] or deconvolutive strategies[3] have been developed. Herein we introduce the principles and describe preliminary studies towards the implementation of an alternative approach, termed *dual recursive deconvolution* (DRED), that draws its strengths from both chemical self-encoding techniques and deconvolution strategies. DRED operates through the iterative identification of the first and last randomized positions of the active members of combinatorial libraries generated through split synthesis. The last building block can be readily obtained from pool screening after the last coupling of the split synthesis, while the first position can be "encoded" by the unique vibrational "fingerprint" of the resin beads used. Once the first and last positions are identified, the second and second to last positions are subjected to the same deconvolution process. Remarkably, this exercise would dramatically simplify the synthetic *and* screening efforts (Supporting Information). For instance, the preparation and DRED of a 64-million hexapeptide library would barely double the number of chemical steps required for the split synthesis of the library (246 versus 120) and would involve only 20 spectroscopically distinguishable beads (DRED beads). Because the matrix is an encoding element of the DRED strategy, libraries can be evaluated while still attached to the bead or close to the beads from which they were released.

The suitability of a near-infrared Raman imaging (NIRIM) instrument[4] as a tool for the simultaneous identification of beads of various chemical composition was investigated. The NIRIM uses fiber-bundle image compression (FIC) technol-

[*] Prof. Dr. H. Fenniri, Dr. H. G. Hedderich, Dr. K. S. Haber, J. Achkar, B. Taylor, Prof. Dr. D. Ben-Amotz
1393 H. C. Brown Laboratory of Chemistry
Purdue University
West Lafayette, IN 47907-1393 (USA)
Fax: (+1) 765-494-0239
E-mail: hf@purdue.edu

[**] This work was supported by Purdue University, the TRASK fund, and the National Science Foundation (CHE-9875390 to HF, DMR-9704162 to DB). HF is a Cottrell Scholar of Research Corporation. DRED = dual recursive deconvolution.

Supporting information for this article is available on the WWW under http://www.wiley-vch.de/home/angewandte/ or from the author.

ogy[5] to simultaneously collect a three dimensional (3D) Raman spectral-imaging data cube ($\lambda$-x-y) containing an optical spectrum ($\lambda$) at each spatial location (x-y) of a globally illuminated area. It should be noted that this is a real-time imaging technique as opposed to the previously reported step-scan methods,[6] which require much longer to generate an image of the sample.

Vital to the success of the DRED method is the ability to identify resin beads based on their polymeric constituents and regardless of the chemical nature of their cargo. To address this dilemma, samples of 18 Merrifield-resin beads carrying various protected amino acids were positioned in the field of view of the NIRIM and single-bead Raman spectra were recorded between 100 $cm^{-1}$ and 1900 $cm^{-1}$.[7] Visual inspection of these spectra indicated that the spectral features were dominated by the matrix (polystyrene (PS)) and even background subtraction (unsubstituted PS beads) did not reveal the spectral features of the loaded material. Hence, Raman imaging of PS-supported compounds is insensitive to the material loaded on the beads at least up to 1.0 mmol of the amino acids studied per gram of resin.[7] Interestingly, while the spectral features of the loaded material become detectable at much higher loadings the resin vibrations and their intensity remain essentially unaffected. An extreme illustration of this result is displayed by TentaGel beads, which are 30/70 (w/w) PS/polyethyleneglycol (PEG) graft copolymer. The Raman spectrum of TentaGel shows vibrations specific to the PEG component as well as the fingerprint transitions of PS which have not been affected by the PEG component (compare Figure 1A and 1C). In addition, the Raman spectra of PS and TentaGel-S-OH beads displayed unique vibrations that were used to image and identify them selectively. Figure 1B shows a $5 \times 5$ FIC frames Raman image of a mixture of PS- and TentaGel-resin beads (exposure time of 45 seconds per frame, total scan time 20 minutes).[8] The classified images (Figure 1D–F) were readily derived from the Raman data using the spectral angle mapper (SAM) algorithm of the spectral-imaging software package MultiSpec.[9] Transitions at 1277 $cm^{-1}$ for TentaGel-S-OH (Figure 1D) and at 1000 $cm^{-1}$ and 1031 $cm^{-1}$ for PS (Figure 1F) were used to identify the corresponding beads. Figure 1E is an image where both PS and TentaGel beads were specifically and concomitantly identified.

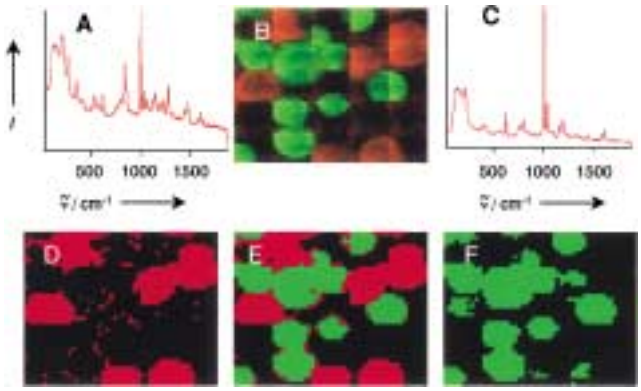


Figure 1. Experiments showing that the vibrations of the PS portion of TentaGel remains essentially unaffected by the major component (PEG) of the bead. Raman spectra of TentaGel-S-OH (A) and polystyrene (C) resin beads. $5 \times 5$ FIC frames Raman image ($50 \times 40$ FIC fibers and $15 \times 12$ μm per single image-pixel) of a mixture of polystyrene and TentaGel-S-OH recorded with a $10\times$ objective, a global illumination laser power of $\approx$400 mW per single frame region and a single frame detector integration time of 45 seconds (B).[8] Classification images[9] of TentaGel-S-OH (D), polystyrene (F) and a mixture of both resin beads (E) produced from the NIRIM image B.

To further extend our ability to reliably identify resin beads based on unique differences in their chemical nature, we have studied the following PS- and non-PS-based resins: (a) 4-bromo-PS, (b) 4-carboxy-PS, (c) PEG cross-linked Merrifield (PS) resin, (d) amino-PEGA, (e) HMBA-SPAR 50 and (f) SPAR 50. Figure 2 shows $5 \times 5$ frames ($50 \times 40$ pixels) and $6 \times 6$ frames ($60 \times 48$ pixels) in which all the beads were identified following the same procedure as in Figure 1. Resins a–c were chosen to establish that at least three additional PS-based resins can be readily distinguished (Figure 2A). Resins d–f were chosen to establish the identification of polyamide-based supports (Figure 2F), and to demonstrate that they can be readily differentiated from PS-based beads (Figure 2C, 2D, and 2F–H). The images in Figure 2 were obtained by combining 1 mg of each of the resins in

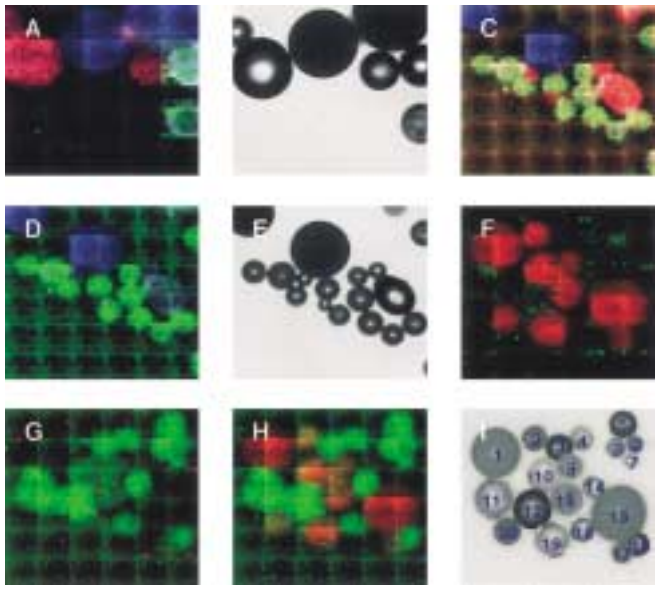


Figure 2. Series of experiments demonstrating the high reliability of multispectral imaging in identifying beads based on their polymeric constituents. The images were obtained from a statistical mixture of six different beads (see text). A) Specific NIR-Raman imaging of 4-bromo-PS (blue, 1073 $cm^{-1}$), 4-carboxy-PS (green, 637 $cm^{-1}$), and PEG cross-linked PS (red, 703 $cm^{-1}$). B) White-light image of the beads in A. C) Specific NIR-Raman imaging of 4-bromo-PS (blue), 4-carboxy-PS (green), and HMBA-SPAR 50 (red, 854 $cm^{-1}$). D) Same image as in C, but only the beads with a PS backbone are visualized. In addition, the two PS-based resins were color coded using vibrations specific to each of them (4-bromo-PS, blue, 4-carboxy-PS, green). E) White-light image of the beads in C and D. F) Specific near IR-Raman imaging of PS based resins (red, 4-bromo-PS, 4-carboxy-PS, PEG cross-linked-PS). G) Specific NIR-Raman imaging of polyamide based resins (green, amino-PEGA, HMBA-SPAR 50, SPAR 50). H) NIR-Raman image where PS- and polyamide-based resins were selectively and concomitantly identified. I) White-light image of the beads in F–H. All the beads were identified by multispectral imaging as well as by single-bead microspectroscopy (4-bromo-PS: beads No. 1 and 15; 4-carboxy-PS: beads No. 9, 10, 13, 19; PEG cross-linked-PS: beads No. 2, 17, 20; amino-PEGA: beads No. 3, 5, 12, 16; HMBA-SPAR 50: beads No. 4, 11, 14, 18; SPAR 50: beads No. 6, 7, 8).

  1433-7851/00/3924-4484 $ 17.50+.50/0 

methanol, a drop of this suspension was then deposited on a sapphire. After evaporation of the solvent the sapphire was placed in the field of view of the NIRIM. A library of single-bead NIR–Raman spectra of each of the resins was first recorded (Supporting Information), then several regions were arbitrarily selected for multispectral imaging. Since each bead appears as a collection of pixels and each pixel is a NIR–Raman spectrum of that area of the bead, comparison of these pixel spectra with the library of single-bead spectra recorded on the authentic samples confirmed the automated assignments. These results were reproducible regardless of the size and shape of the beads (Supporting Information).

The principles of dual recursive deconvolution of resin-supported combinatorial libraries have been proposed and the feasibility of the key feature of this method, the identification of the first randomized position, has been demonstrated using NIR-Raman imaging of self-encoded resin beads. The reliability of this method is very high, it has been consistently accurate over the two and a half years that we have been practicing multispectral imaging. Furthermore, any imaging technique could be applicable to the DRED method as long as the beads used display unique spectral features, and provided the loaded material does not significantly alter their spectral signature. For instance, secondary-ion mass spectrometry (SIMS)[10] and FT-IR[11] imaging are alternative approaches that we are investigating. Although, several commercially available and chemically distinct solid supports are eligible to explore the scope of DRED in combinatorial chemistry, inhomogeneities in their physical and chemical properties (e.g. swelling, porosity, size, reactivity) prompted the design of the DRED beads, a new class of resins for solid-phase synthesis.[12] The added value of the DRED method is that it is a non-invasive screening technique, it does not necessarily require sophisticated equipment, it is inexpensive, and it does not involve the development of any encoding chemistry since the DRED beads will soon become commercially available.

Received: August 4, 2000 [Z15581]

[1] Á. Furka, L. K. Hamaker, M. L. Peterson in *Combinatorial Chemistry: A Practical Approach* (Ed.: H. Fenniri), Oxford University Press, Oxford, **2000**, pp. 1–32.

[2] a) W. C. Still, *Acc. Chem. Res.* **1996**, *29*, 155–163; b) W. L. Fitch, T. A. Baer, W. Chen, F. Holden, C. P. Holmes, D. MacLean, N. Shah, E. Sullivan, M. Tang, P. Waybourn, S. M. Fisher, C. A. Miller, L. R. Snyder, *J. Comb. Chem.* **1999**, *1*, 188–194; c) M. C. Needels, D. G. Jones, E. H. Tate, G. L. Heinkel, L. M. Kochersperger, W. J. Dower, R. W. Barrett, M. A. Gallop, *Proc. Natl. Acad. Sci. USA* **1993**, *90*, 10700–10704; d) K. S. Lam, M. Lebl, V. Krchnak, *Chem. Rev.* **1997**, *97*, 411–448; e) X.-Y. Xiao, K. C. Nicolaou in *Combinatorial Chemistry: A Practical Approach* (Ed.: H. Fenniri), Oxford University Press, Oxford, **2000**, pp. 75–94.

[3] a) A. Nefzi, J. M. Ostresh, R. A. Houghten, *Chem. Rev.* **1997**, *97*, 449–472; b) D. L. Boger, W. Chai, Q. Jin, *J. Am. Chem. Soc.* **1998**, *120*, 7220–7225; c) M. C. Pirrung, J. Chen, *J. Am. Chem. Soc.* **1995**, *117*, 1240–1245.

[4] A. D. Gift, J. Ma, K. S. Haber, B. L. McClain, D. Ben-Amotz, *J. Raman Spectrosc.* **1999**, *30*, 757–765. The NIRIM instrument is currently housed in the Purdue University Laser Laboratory within the Chemistry Department. Web: http://www.chem.purdue.edu/lfac/laser.html

[5] J. Ma, D. Ben-Amotz, *Appl. Spectrosc.* **1997**, *51*, 1845–1848.

[6] a) P. J. Treado, M. D. Morris, *Appl. Spectrosc. Rev.* **1994**, *29*, 1–38; b) G. J. Puppels, M. Grond, J. Greve, *Appl. Spectrosc.* **1993**, *47*, 1257; c) L. Markwort, B. Kip, E. D. Silva, B. Roussel, *Appl. Spectrosc.* **1995**, *49*, 1411–1430.

[7] 90 μm diameter polystyrene (PS; 1% divinyl benzene(DVB)/PS) and 130 μm TentaGel-S-OH resin beads (Advanced ChemTech). See Supporting Information for the list of resin-supported amino acids studied. A detailed description of the design and operation of the NIRIM, and the processing software can be found in ref. [4] and in the Supporting Information.

[8] This acquisition time could be decreased by at least an order of magnitude with a more powerful laser source and a more efficient optics setup.

[9] "MultiSpec—A Tool for Multispectral Image Data Analysis": L. Biehl, D. Langrebe, Pecora 13, Sioux Falls, SD, **1996**. The software can be downloaded at: http://dynamo.ecn.purdue.edu/~biehl/multispec/. See Supporting Information.

[10] C. L. Brummel, J. C. Vickerman, S. A. Carr, M. E. Hemling, G. D. Roberts, W. Johnson, D. Gaitanopoulos, S. J. Benkovic, N. Winograd, *Anal. Chem.* **1996**, *68*, 237–242.

[11] H. Fenniri, J. Achkar, unpublished work.

[12] H. Fenniri, PCT 60/180,939.

## Polymorphism in *p*-Hydroxybenzoic Acid: The Effect of Intermolecular Hydrogen Bonding in Controlling Proton Order versus Disorder in the Carboxylic Acid Dimer Motif**

Benson M. Kariuki, Clare L. Bauer, Kenneth D. M. Harris,* and Simon J. Teat

The phenomenon of polymorphism[1–3] is of considerable contemporary interest in the field of organic solid-state chemistry, in part because comparisons between the properties of polymorphs provide an ideal basis on which to understand relationships between solid-state properties and crystal structure. Furthermore, in the quest to develop reliable computational techniques to predict the crystal structure(s) formed by a given type of organic molecule,[4–8] studies of polymorphic systems provide stringent challenges for assessing the success of these methods. In general, the fact that the structures of organic molecular crystals usually arise from the interplay of several factors of comparable importance leads to intrinsic difficulties in attempting to predict and/or rationalize such structures. However, when one type of intermolecular interaction (or a small number of interactions) is dominant, a reliable rationalization of the observed molecular packing

[*] Prof. Dr. K. D. M. Harris, Dr. B. M. Kariuki, Dr. C. L. Bauer
School of Chemistry, University of Birmingham
Edgbaston, Birmingham B15 2TT (UK)
Fax: (+44) 121-414-7473
E-mail: K.D.M.Harris@bham.ac.uk
Dr. S. J. Teat
CCLRC Daresbury Laboratory
Daresbury, Warrington, Cheshire WA4 4AD (UK)

[**] We are grateful to the EPSRC and Daresbury Laboratory for financial support (CASE award to C.L.B.) and for the award of beam-time at Daresbury Laboratory.

  1433-7851/00/3924-4485 $ 17.50+.50/0 